JOURNAL OF SOLID STATE CHEMISTRY **141,** 205–211 (1998)
ARTICLE NO. SC987954

A New High-Pressure Modification of Nb_2O_5

I. P. Zibrov,* V. P. Filonenko,† P.-E. Werner,‡ B.-O. Marinder,‡ and M. Sundberg‡,[1]

*Institute of Crystallography, Russian Academy of Sciences, 117 333 Moscow, Russia; †Institute for High Pressure Physics, Russian Academy of Sciences, Troitsk, 149092 Moscow region, Russia; ‡Department of Inorganic and Structural Chemistry, Arrhenius Laboratory, Stockholm University, S-106 91 Stockholm, Sweden

Received December 24, 1997; in revised form June 26, 1998; accepted July 6, 1998

The transformation of H-Nb_2O_5 has been studied by using a "toroid"-type high-pressure chamber at pressures of 5.0 and 8.0 GPa in the temperature region 800–1400°C. A mixture of B-Nb_2O_5 and a new modification of niobium pentoxide (denoted Z-Nb_2O_5) with seven-coordinated niobium was found in the samples after treatment at $P = 8.0$ GPa, $T = 800$–1100°C for 1–10 min. The structure was determined and refined by the Rietveld method from X-ray powder diffraction data. The thermogravimetric analysis showed no reduction of the sample.

INTRODUCTION

Previous investigations of the relationships between pressure, temperature, and structure have shown that B-Nb_2O_5 and T-Nb_2O_5 are high-pressure modifications of Nb_2O_5. The latter, T-Nb_2O_5, is considered to be the stable high-pressure, high-temperature modification (1–3). By using three types of high-pressure apparatus: piston cylinder-type ($P \approx 0.5$–2 GPa), belt-type ($P \approx 3$–6 GPa), and Bridgman-type (P ≈ 15 GPa), Tamura (1) observed that H-Nb_2O_5 transformed first to B-Nb_2O_5 and then to T-Nb_2O_5 with increasing temperature at constant pressure. He also found direct transitions from H-Nb_2O_5 to B-Nb_2O_5 and from H-Nb_2O_5 to T-Nb_2O_5 under the following PT-conditions: $P = 15$ GPa, $T = 300$°C and $P = 0.5$ GPa, $T > 1000$°C, respectively.

Shock-loading experiments on single crystals of H-Nb_2O_5 were made in the pressure range 5–50 GPa by using a gun method, leading to a complete transformation from H-Nb_2O_5 to T-Nb_2O_5 at $P > 15$ GPa (4,5). In addition to T-Nb_2O_5 and Nb_xO_2 (rutile-type), a new phase (denoted X) was observed in some of the experiments ($P > 40$ GPa). A high-resolution image of the X-phase was interpreted as a two-dimensionally disordered H-Nb_2O_5 structure.

[1] Corresponding author. E-mail: marsu@inorg.su.se.

The goal of the present work was to investigate the phase transformations of H-Nb_2O_5 at $P \approx 8.0$ GPa by using the high-pressure synthesis method developed for the tungsten-oxygen system. In this system five new high-pressure tungsten oxides, W_3O_8(I), W_3O_8(II), $WO_{2.625}$, $WO_{2.5}$, and WO_2(hp), have been prepared from mixtures of W and WO_3 powders ($T = 900$–1300°C and $P = 5.0$–8.0 GPa) (6–9).

SYNTHESIS METHOD

A single-phase powder of H-Nb_2O_5 was prepared by heating Nb_2O_5 (99.9% purity) in air at 1050°C for 1 h. The powder was pressed into pellets of dimensions: 4mm in height, 5mm in diameter, which were then wrapped up in Pt or Mo foils to avoid chemical reactions between the specimen and the surrounding cell material.

The experiments were carried out in a high-pressure chamber of "toroid"-type (10), consisting of two hard metal anvils of a special profile. The pressure was generated in a lithographic limestone cell (Fig. 1) placed between the anvils. The tube-type graphite heater, located inside the limestone cell, was heated by an electric current. The pressure values were calibrated by measuring the electric conductivity of Bi and Ba at room temperature (transitions; Bi I–II at 2.55 GPa and Bi IV–V at 7.7 GPa) and Ba I–II at 5.5 GPa. The temperature was measured by three W-Re thermocouples placed in different parts of the cell. The temperature gradient along the sample height was found to be less than 50°C. The correlation between the electric power fed to the heater and the sample temperature was determined for the pressures 5.0 and 8.0 GPa and used in the experiments below.

The high-pressure syntheses were performed under the following experimental conditions: $P = 5.0$ GPa, $T = 900$°C and 1000°C (two samples); $P = 7.5$–8.0 GPa and $T = 800$–1400°C (14 samples) (see Fig. 2). The applied pressure stabilized after 12–15 min, and the specimen was then heated to the wanted temperature, which was held for 1–10 min. Thereupon, the sample was quenched to room temperature at a rate of ~ 100°C/s before the pressure was released.

0022-4596/98 $25.00

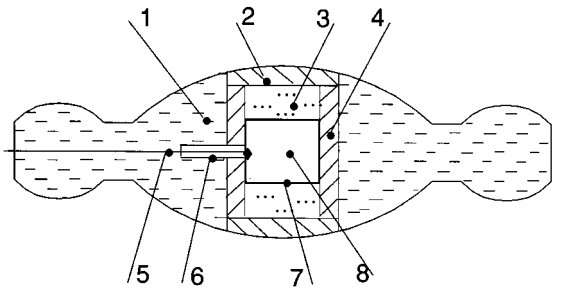

FIG. 1. A model showing the filled high-pressure cell: 1, limestone cell; 2, graphite covers; 3, BN covers; 4, graphite heater; 5, thermocouple; 6, Al_2O_3 tube; 7, Pt foil; 8, sample.

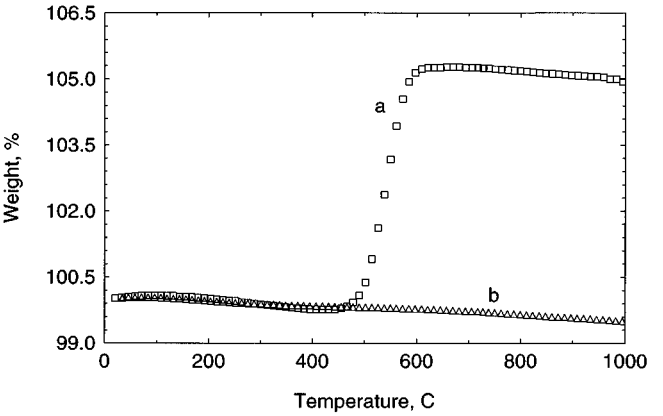

FIG. 3. Thermogravimetric analysis data for the products: (a) NbO_2 obtained at $P = 8.0$ GPa, $T = 1400$°C; (b) two-phase sample of the B and Z modifications of Nb_2O_5 obtained at $P = 8.0$ GPa, $T = 1000$°C.

X-RAY DIFFRACTION AND THERMAL ANALYSIS STUDIES

X-ray powder photographs of all samples were taken in a subtraction-geometry Guinier–Hägg focusing camera, with strictly monochromatized Cu$K\alpha_1$ radiation. Si was used as the internal standard.

The X-ray results, summarized in Fig. 2, show that B-Nb_2O_5 was prepared at $P = 5.0$ GPa, ($T = 900$°C and 1000°C) and that a mixture of B-Nb_2O_5 and an unidentified phase (denoted Z below) was formed at $P = 7.5$–8.0 GPa and $T = 800$–1100°C. The previously reported high-pressure, high-temperature modification (T-Nb_2O_5) was found in the samples prepared at $T = 1250$°C, $P = 7.5$ GPa and $T = 1300$°C, $P = 8.0$ GPa. At still higher temperatures, $T > 1350$°C, oxygen was lost from the starting material, resulting in the formation of NbO_2, which was confirmed from its X-ray powder pattern.

Thermogravimetric analysis (TGA) studies were made on two samples in a Perkin Elmer TGA7 apparatus. The TGA run of a sample consisting of B-Nb_2O_5 and the unknown Z-phase (Fig. 3) showed that heating in oxygen caused no weight increase. This means that the stoichiometry of the sample is almost exactly Nb_2O_5 and the unknown phase is thus regarded as a new modification of Nb_2O_5. The X-ray powder patterns obtained from the starting sample and the final product after the TGA run are shown in Fig. 4. The latter product was identified as consisting of a mixture of B-Nb_2O_5 and T-Nb_2O_5. It can therefore be concluded that the new Nb_2O_5-modification is less stable than the B and T forms when heated at ambient pressure. The amount of Z-Nb_2O_5 in the two-phase samples depended on the experimental conditions (T, and time). The maximum content of Z-Nb_2O_5 in the samples was ~50%. After the high-pressure synthesis the samples had a white color with a touch of gray, which also supports the assumption of an Nb_2O_5 composition for the Z-modification. The samples were very soft and could be easily crushed in a mortar. The oxygen

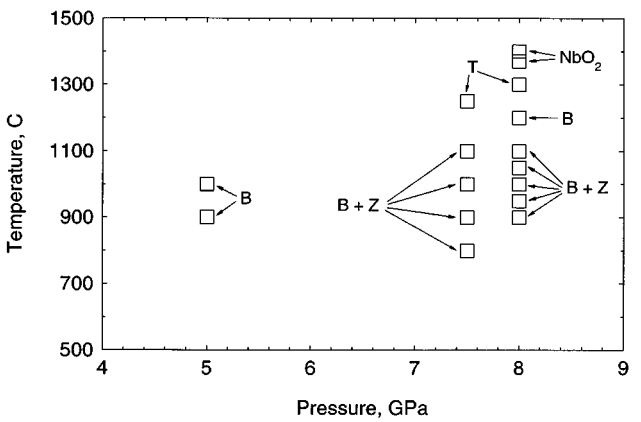

FIG. 2. Temperature/pressure relationships for B, T, and Z-forms of Nb_2O_5 as found in the present work.

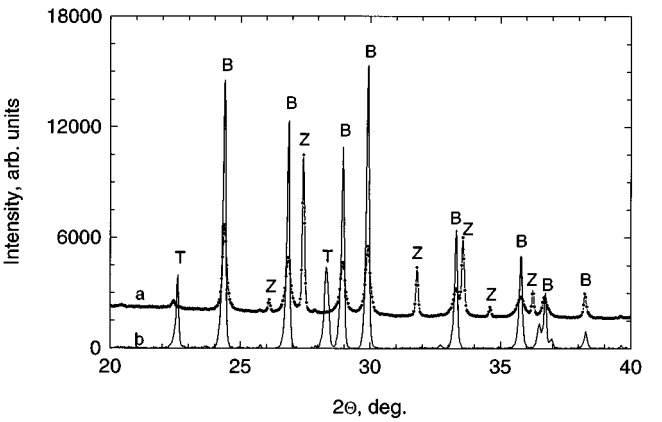

FIG. 4. (a) X-ray powder pattern of the two-phase sample in Fig. 3b. (b) X-ray powder pattern of the same sample after running it in O_2 atmosphere in the TGA apparatus.

content of the NbO_2 product was confirmed by thermogravimetric analysis (Fig. 3).

STRUCTURE DETERMINATION

An X-ray powder diffraction photograph indicated a two-phase sample of B-Nb_2O_5 and the Z-phase and was tentatively indexed in the following way. The lines from B-Nb_2O_5 were subtracted from the X-ray pattern. From the remaining lines a *C*-centered cell of the Z-phase was found by the autoindexing program Treor90 (11). As several lines from the two phases overlap, the unit cell dimensions reported in Table 1 are taken from the result of a two-phase Rietveld refinement based on powder diffractometer data.

X-ray diffraction data for structure determination and refinement were collected on a Stoe Stadi/P diffractometer with a rotating sample in symmetric transmission mode. A symmetric focusing germanium monochromator (focal distance = 440 mm) was used to give pure Cu$K\alpha_1$ radiation ($\lambda = 1.540598$ Å). The diffraction data were collected with a small linear-position sensitive detector (PSD) covering 6.4° in 2θ. The PSD was moved in steps of 0.2°, 400 s/step, thus giving an average intensity of 32 measurements at each 2θ position. It has been found that the angular resolution of the diffractometer operated under these conditions is approximately the same as that of a Guinier–Hägg photograph. The 2θ range measured was $8^\circ < 2\theta < 95^\circ$. The peak shapes may be described by a symmetric pseudo-Voigt function.

A neutron diffraction pattern ($\lambda = 1.4700$ Å) was collected at the Swedish research reactor in Studsvik. A rather large amount of sample was needed for this data collection, however, and it was not possible to synthesize the quantity needed without an appreciably lower percentage of the Z-phase in the sample. Furthermore, the lines were very broad.

TABLE 1
Crystal Data for Z–Nb_2O_5 and Data from the Final Rietveld Refinements

Space group	*C*2
Z	2
F.W. (at 298 K)	265.78
a(Å)	5.2193(2)
b(Å)	4.6995(2)
c(Å)	5.9285(2)
β(°)	108.559(2)
V(Å^3)	137.85
d-calc. (g/cm^3)	6.40
R_F	0.048
R_P	0.067
R_{WP}	0.089
d	0.17
$FWHM_{min}$(°)	0.086
$FWHM_{max}$(°)	0.158

Note. *d* = Durbin–Watson statistic *d*-value according to Hill and Flack (20).

TABLE 2
Z–Nb_2O_5 Position Parameters in Space Group *C*2

Atom	Site	*x*	*y*	*z*
Nb	(4c)	0.2101(4)	0.0	0.2654(4)
O1	(4c)	0.159(3)	0.174(3)	0.937(3)
O2	(4c)	0.076(3)	0.673(3)	0.306(3)
O3	(2b)	0.0	0.218(4)	0.5

From systematic absences it was found that Z-Nb_2O_5 crystallizes in space group *C*2, *Cm*, or *C*2/*m*. The final structure determination was made in *C*2. The unit cell parameters are given in Table 1. As the unit cell volume is very small, the structure was determined by trial-and-error. Although the neutron diffraction data material from the two-phase sample was of rather low quality, it was used for preliminary determination of the oxygen positions. In the final Rietveld refinement the smallest standard deviations were obtained with the X-ray data, and the positional coordinates reported in Table 2 are therefore taken from this refinement. The Rietveld program used was a local version of the program DBW3.2S (12). The positional coordinates for B-Nb_2O_5 taken from (13) were held fixed during refinement.

Although the final structure factor R-value for Z-Nb_2O_5 is 0.048, there are strong indications that the refined positional parameters listed in Table 2 are of low quality. Thus, for example, the Bérar–Lelann test (14) for serial correlation indicated that the STDs should be multiplied by a factor of 5.7. One reason for this large factor is that a few lines from an unknown impurity phase are clearly seen in the diffraction pattern. The strongest unidentified lines can be seen at $2\theta = 22.44^\circ$ and 49.16° (see Fig. 5). The presence of the impurity may have a destructive influence on the parameters obtained from the Rietveld refinement. It should be noted that reflections from Z-Nb_2O_5 are narrower than the B-phase reflections (cf. Fig. 5). Some oxygen–oxygen distances are obviously too short according to normal standard (see Table 3), but it should be noted that the volume per oxygen atom in Z-Nb_2O_5, 13.8 Å^3, is exceptionally small.

Although the positional coordinates must be judged with caution, the general Nb-O coordination in the structure is revealed. A structure model can be seen in Fig. 6a. The structure is built up of two layers of oxygen atoms at $y \approx 0.17$ and $y \approx 0.67$. The O_3 atoms deviate somewhat from these values. The oxygen arrangement within these layers is very similar to that in another high-pressure phase,

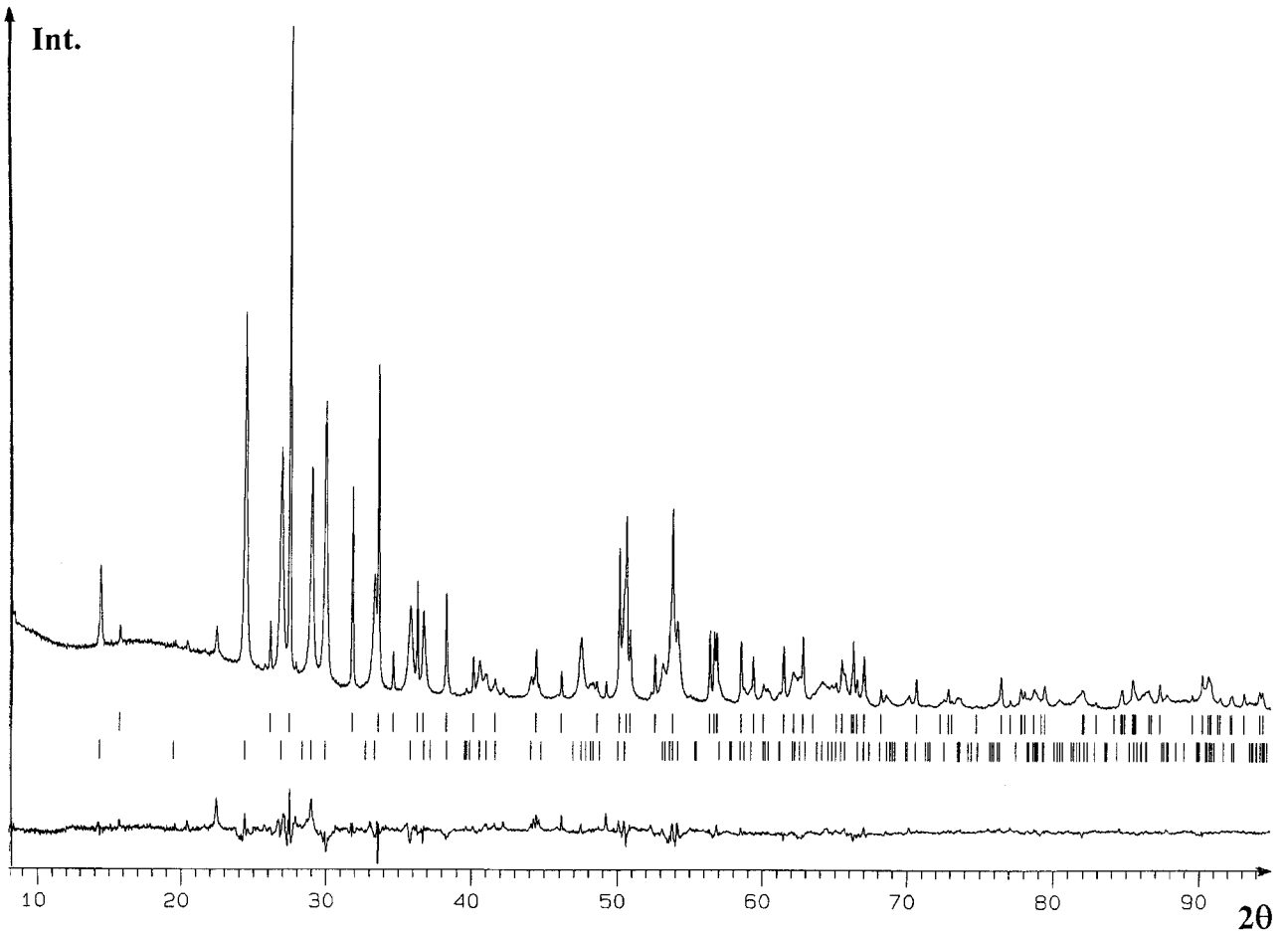

FIG. 5. X-ray Rietveld refinement of Z-Nb_2O_5. The upper curve illustrates the observed data, and the lower is the difference between observed and calculated data. The positions of all allowed Bragg reflections are indicated by the rows of vertical tick marks: Z-Nb_2O_5, upper; B-Nb_2O_5, lower.

namely W_3O_8(I) (Fig. 6b), as may be seen from the oxygens in or near the plane containing tungsten (6). Then, as a consequence of the *C*-centering in Z-Nb_2O_5, the niobium atoms (at $y = 0$ and 0.5) are coordinated by four oxygens in or near one plane above and by three oxygens in or near a parallel plane below, giving an irregular coordination of seven oxygens around niobium (Fig. 6c). The oxygen arrangement of Z-Nb_2O_5 parallel with (0 1 0) is, as mentioned above, similar to a part of that in W_3O_8(I) whose structure is isotypic with the Andresen's model of U_3O_8. It has been shown that this model constitutes an integrating part of T-Nb_2O_5 (15) as indicated in Fig. 6b. In this way the model of the Z-Nb_2O_5 structure as described here is related to T-Nb_2O_5.

A similar kind of seven-coordination as found for Z-Nb_2O_5 has been observed in the mineral baddeleyite, ZrO_2 (16), and in $Nb_2Zr_6O_{17}$ (17). ZrO_2 is isostructural with NbON (18) and has been described as built up of monocapped trigonal prisms (19). The same type of coordination polyhedra can also be found in Z-Nb_2O_5 by considering layers of oxygens *A* and *B* in or near planes parallel with $(2\,0\,\bar{1})$ as indicated in Fig. 6c. Layers *A* and *B* alternate in an *hcp* sequence. In Fig. 6c two monocapped trigonal prisms are shown with a common edge. It is noteworthy that there is a similar oxygen arrangement in the B-Nb_2O_5 modification with the oxygens in a slightly distorted *hcp* array. The niobium atoms, however, reside, not in trigonal prisms, but in pairs of octahedra with a common edge.

TABLE 3
Selected Interatomic Distances (Å) in Z–Nb_2O_5

Nb–Nb	3.21	O1–O1	2.02	O2–O2	2.52
		O1–O1′	2.56	O2–O3	2.87
Nb–O1	2.05	O1–O1″	2.56	O2–O3′	2.15
Nb–O1′	2.08	O1–O2	2.82		
Nb–O1″	2.18	O1–O2′	2.82	O3–O3	> 3.0
Nb–O2	1.74	O1–O2″	2.55		
Nb–O2′	2.02	O1–O2‴	2.29		
Nb–O3	2.27	O1–O3	2.46		
Nb–O3′	2.15				

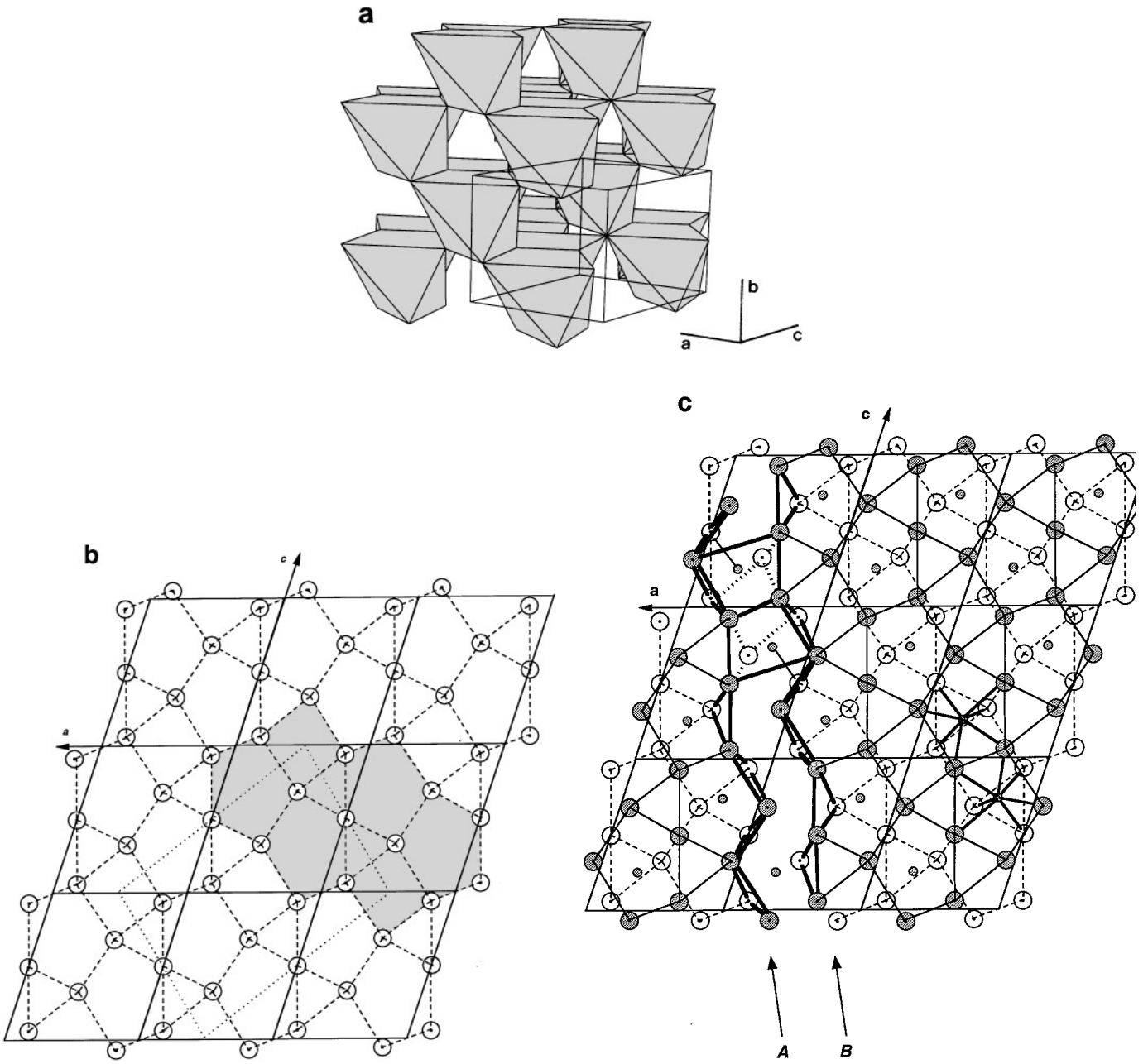

FIG. 6. (a) Crystal structure of Z-Nb_2O_5. Note the irregular polyhedra of seven-coordinated niobium. The drawings are produced with ATOMS by Shape Software. (b) Bounded projection along the *b*-axis with $0.17 < y < 0.22$ showing one net (dashed) of oxygen atoms in Z-Nb_2O_5. Note the similarity with an oxygen layer of W_3O_8(I). The dotted, not oblique unit-cell of W_3O_8(I) indicates a slight distortion of the orthorhombic W_3O_8 layer as compared with that of Z-Nb_2O_5. Shaded polygons show part of the oxygen arrangement in T-Nb_2O_5. (c) Bounded projection along the *b*-axis showing two nets of oxygen atoms with $y \approx 0.17$ (dashed) and $y \approx 0.67$ (continuous) and with niobium atoms at $y = 0.5$. Two niobium atoms bonded to oxygens are shown to the right. To the left two oxygen layers, *A* and *B*, are indicated in heavy outline parallel with $(20\bar{1})$. More or less distorted trigonal prisms are formed between these layers. Two monocapped trigonal prisms with a common edge shown to the upper left in the figure.

ELECTRON MICROSCOPY STUDY

A high-resolution electron microscopy (HREM) study of a few samples has been started. The HREM specimens were prepared by crushing a small amount of a sample in an agate mortar and dispersing the resultant fragments in *n*-butanol. A few drops of the suspension were put on a holey carbon film supported on a Cu-grid. The grid was then examined in JEOL 200CX and JEOL 3010 transmission electron microscopes fitted with double-tilt goniometer

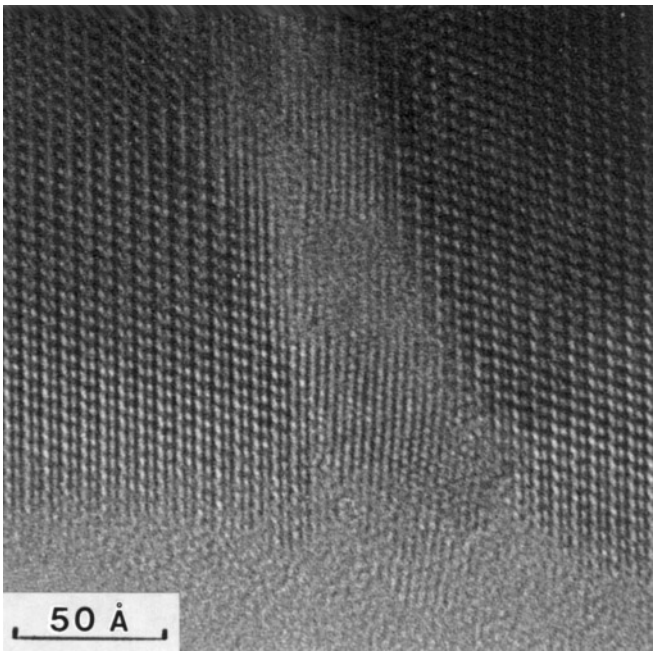

FIG. 7. Low-magnification image of B-Nb_2O_5 in (010) projection. The unit cell dimensions of B-Nb_2O_5 are $a = 12.730$, $b = 5.560$, $c = 4.880$ Å, and $\gamma = 105.05°$ (13). A defect region in the middle of the micrograph can also be seen.

stages and operated at accelerating voltages of 200 kV and 300 kV, respectively.

The first results show well-ordered, as well as twinned and heavily disordered crystals of B-Nb_2O_5. It should be noted that it has not yet been possible to find a crystal fragment of Z-Nb_2O_5. However, the low-magnification micrograph of a B-Nb_2O_5 crystal projected along the 5.5-Å axis (Fig. 7) shows a small area with a different contrast in the middle of the image. This might indicate that a small region of Z-Nb_2O_5 is intergrown with the B-Nb_2O_5 phase on both sides. Such crystals were frequently observed. Previous observations made on the two high-pressure phases of W_3O_8 compositions have shown that small regions of W_3O_8(I) are intergrown with larger regions of W_3O_8(II) on both sides (6). W_3O_8(I) has a higher density than the latter phase, which is also in agreement with the observations made on the niobium oxides.

CONCLUDING REMARKS

This investigation has shown that H-Nb_2O_5 transforms to B-Nb_2O_5 and to T-Nb_2O_5 with increasing temperature and pressure. These results are in agreement with previous temperature–pressure phase relationships studies on Nb_2O_5 (1–3). Besides the known high-pressure phases, we have observed a new high-pressure modification of Nb_2O_5, denoted Z-Nb_2O_5, in two-phase samples (B and Z modifications) synthesized at $P \approx 7.5 - 8$ GPa and $T =$ 800–1100°C. Thermal analysis studies showed the new Z-form to be less stable than both the B- and T-modifications. Our results also show that Z-Nb_2O_5 and the previously reported X-phase (4) represent different structures.

The niobium atoms are six-coordinated (NbO_6-octahedra) in B-Nb_2O_5 and seven-coordinated in Z-Nb_2O_5. The stable high-pressure and high-temperature modification, T-Nb_2O_5, contains six- and seven-coordinated niobium atoms in the form of slightly distorted NbO_6-octahedra and pentagonal NbO_7-bipyramids in the structure (3). Although the latter coordination polyhedron differs from that in Z-Nb_2O_5, there are also striking similarities between these two phases as described above. It should be noted that an increase of the coordination number is favored by high pressure. A HREM study of the relationships between T-Nb_2O_5, B-Nb_2O_5, and Z-Nb_2O_5 is under way. Of special interest are the disordered and intergrowth structures.

ACKNOWLEDGMENTS

This study has partly been performed within a program for Swedish–Russian joint research projects supported by the Royal Swedish Academy of Sciences and by a Visiting Scientist Grant from the Royal Swedish Academy of Sciences through its Nobel Institute for Chemistry. This support is gratefully acknowledged. We want to thank Dr. R. McGreevy at NFL, Studsvik, for providing the facilities for the neutron diffraction work and Mr. H. Rundlöf for collection of the neutron diffraction data. The research described here was made possible in part by Grant N95-03-08146a from the Russian Foundation of Fundamental Investigations. Financial support from the Swedish Natural Science Research Council is also gratefully acknowledged.

REFERENCES

1. S. Tamura, *J. Mater. Sci.* **7,** 298 (1972).
2. J. L. Waring, R. S. Roth, and H. S. Parker, *J. Res. Natl. Bur. Stand. (U.S.) A* **77,** 705 (1973).
3. K. Kato and S. Tamura, *Acta Cryst.* **31,** 673 (1975).
4. M. Kikuchi, K. Kusaba, E. Bannai, K. Fukuoka, Y. Syono, and K. Hiraga, *Jpn J. Appl. Phys.* **24,** 1600 (1985).
5. M. Kikuchi, K. Kusaba, K. Fukuoka, and Y. Syono, *J. Solid State Chem.* **63,** 386 (1986).
6. M. Sundberg, N. D. Zakharov, I. P. Zibrov, Yu. A. Barabanenkov, V. P. Filonenko, and P. Werner, *Acta Cryst. B* **49,** 951 (1993).
7. Yu. A. Barabanenkov, N. D. Zakharov, I. P. Zibrov, V. P. Filonenko, P. Werner, A. I. Popov, and M. D. Valkovskii, *Acta Cryst. B* **49,** 169 (1993).
8. M. Sundberg, P.-E. Werner, and I. P. Zibrov, *Z. Krist.* **209,** 662 (1994).
9. V. P. Filonenko, I. P. Zibrov, and M. Sundberg, "High Press. Sci. and Tech., Proc. Joint XV AIRAPT and XXXIII EHPRG Int. Conf. 1996," p. 110.
10. L. G. Khvostantsev, L. F. Vereshchagin, and A. P. Novikov, *High Temp.–High Pressure* **9,** 637 (1977).
11. P.-E. Werner, L. Eriksson, and M. Westdahl, *J. Appl. Cryst.* **18,** 367 (1985).

12. D. B. Wiles, A. Sakthivel, and R. A. Young, "User's Guide to Program DBW 3.2S for Rietveld Analysis of X-ray and Neutron Powder Diffraction Patterns (Version 8804)." School of Physics, Georgia Institute of Technology, Atlanta.
13. F. Laves, W. Petter, and H. Wulf, *Die Naturwissenschaften* **24,** 633 (1964).
14. J. F. Bérar and P. Lelann, *J. Appl. Cryst.* **24,** 1 (1991).
15. B.-O. Marinder, *Acta Chem. Scand.* **44,** 123 (1990).
16. J. D. McCullough and K. N. Trueblood, *Acta Cryst.* **12,** 507 (1959).
17. J. Galy and R. S. Roth, *J. Solid State Chem.* **7,** 277 (1973).
18. von M. Weishaupt and J. Strähle, *Z. Anorg. Allg. Chem.* **429,** 261 (1989).
19. B. G. Hyde and S. Andersson, "Inorganic Crystal Structures," p. 185, Wiley, New York, 1989.
20. R. J. Hill and H. D. Flack, *J. Appl. Cryst.* **20,** 356 (1987).